Adaptive Control Allocation in the Presence of Actuator Failures

Yu Liu[*] and *Luis G. Crespo*[†]

In this paper, a novel adaptive control allocation framework is proposed. In the adaptive control allocation structure, cooperative actuators are grouped and treated as an equivalent control effector. A state feedback adaptive control signal is designed for the equivalent effector and allocated to the member actuators adaptively. Two adaptive control allocation algorithms are proposed, which guarantee closed-loop stability and asymptotic state tracking in the presence of uncertain loss of effectiveness and constant-magnitude actuator failures. The proposed algorithms can be shown to reduce the controller complexity with proper grouping of the actuators. The proposed adaptive control allocation schemes are applied to two linearized aircraft models, and the simulation results demonstrate the performance of the proposed algorithms.

I. Introduction

Actuation redundancy is highly desirable for fault-tolerant control in aircraft systems. Because of the control effector redundancies, there are multiple ways to produce forces and moments that the flight control system needs to attain stability and satisfactory performance. However, this flexibility can also bring the problem of redundancy management, that is, determining how to allocate the control authority.

Control allocation is one of the common approaches to address this redundancy management problem. The purpose of control allocation is to distribute the control signals to the available actuators to generate desired moments and forces. Some commonly seen control allocation methods include explicit ganging,[1] daisy chaining,[2] pseudo inverse,[3,4] and error and control minimization,[5–9] etc. Explicit ganging solves the control allocation problem by finding a static relation between the desired control moments and forces and the designed control signals. Multiple actuators (e.g., two aileron surfaces) can be combined to generate the desired control effects. It is often applied when it is obvious how to combine the redundant actuators. Daisy chaining is capable of allocating desired control signals in a prioritized fashion. It utilizes the actuators in sequence to generate certain desired control effect. If the current actuator is not capable of providing the required control effect due to, for instance, actuator saturation, the next actuator in the sequence will be selected. The pseudo inverse approach solves a constrained optimization problem to find the allocation of control signals, and actuator saturation and failures can also be accommodated in this approach. Error and control minimization is another common control allocation approach. It can minimize the error between the desired and generated control moments subject to control constraints. A secondary objective can be also added to the optimization problem to solve the control minimization or control sufficiency problem. It can be seen that some of the above control allocation approaches are capable of realizing optimization objectives. Several approaches also have the capability of actuator failure and saturation compensation, provided that the failure or saturation information is available. Thus one obvious drawback of these control allocation approaches is that a failure detection subsystem is inevitable for failure compensation. Furthermore, complex computation is also sometimes required for solving optimization problems.

Adaptive control, on the other hand, does not require the knowledge of the failed control effectors due to its capability of autonomously changing the control parameters according to the remaining control authority. Due to parameter adaptation, it is also able to accommodate for uncertainties in the systems. The past decade has seen tremendous research efforts in adaptive flight control designs capable of failure compensation (see, e.g., [10, 11]). Adaptive control's ability to seamlessly compensate for actuator failures

[*]Postdoctoral Associate, National Institute of Aerospace, Hampton, VA 23666. Member, AIAA.
[†]Senior Research Scientist, National Institute of Aerospace, Hampton, VA 23666. Member, AIAA.

requires that the system's built-in actuation redundancy is sufficient, which is usually characterized by a rank condition on the control gain matrix B of the controlled system.[10,12] To maximize such redundancy, one common approach in multivariable adaptive control is to generate a control signal for each control surface. Such an approach endows the controller with maximum degree of freedom for failure compensation. When certain control surfaces are stuck or have reduced control effectiveness, the remaining control surfaces will adaptively cooperate until a new combination of inputs for the remaining control surfaces is found. This will occur automatically without knowing which surfaces have failed, or when such failures occur. Although the adaptive control approach ensures closed-loop stability and tracking performance, the control allocation is usually not taken into consideration. For instance, separately designed control signals for multiple control surface segments may cancel each other's effects.

The lack of control allocation in the current direct adaptive control framework motivates the research work reported in this paper. In this research, we aim to add a control allocation capability to the current adaptive flight control framework for better redundancy management. In the adaptive control allocation framework, a key step is to combine redundant control surfaces similar to explicit ganging. For each group of combined actuators, we design an adaptive control signal, which is then allocated to each member control surface within the group by an adaptive gain. If there is no uncertain failure occurring in the system, the way the control is allocated is known. If a failure occurs, however, the desirable allocation is not known due to the uncertainties of the failure. To compensate for the uncertainties, the designed control signal will be allocated to the group members adaptively. The structure of the adaptive control allocation framework can be illustrated with the following aircraft pitch control example in Figure 1.

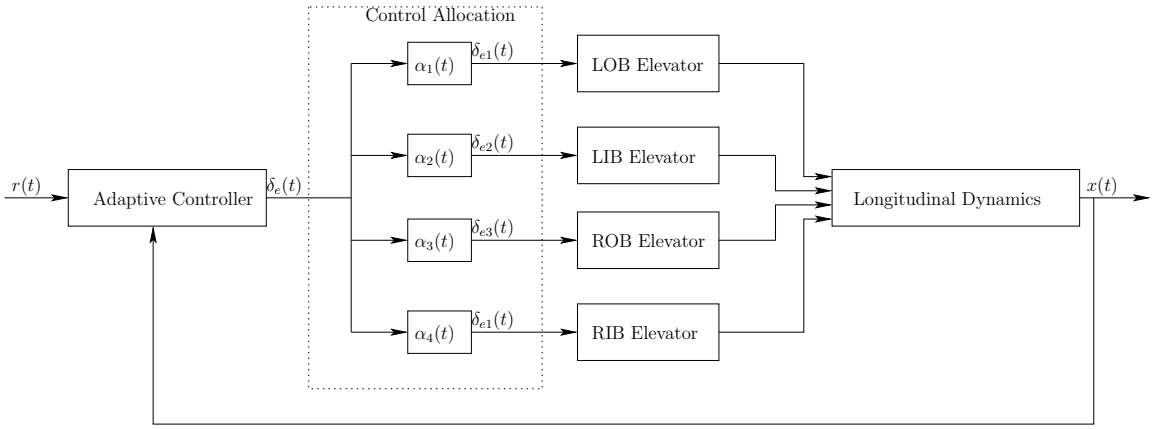

Figure 1. Aircraft pitch control with adaptive control allocation.

This is a simple aircraft control example with the elevator controlling the pitch motion. The aircraft longitudinal state, denoted $x(t)$ in Figure 1, should be tracking a desired trajectory generated by a reference input $r(t)$ and a reference system (which is included in the *Adaptive Controller* block in Figure 1 for simplicity). The elevator consists of four segments, namely left outboard, left inboard, right outboard, and right inboard segments. For pitch control, they can be grouped together and considered as an equivalent elevator. A virtual elevator signal $\delta_e(t)$ is generated from the adaptive controller for desired pitching maneuver. This elevator signal is then allocated by the allocation gains $\alpha_i(t)$, $i = 1, \ldots, 4$. The resulted elevator signals $\delta_{ei}(t)$, $i = 1, \ldots, 4$ will be fed to the four elevator segments. The allocation gains can be updated on-line based on the knowledge of the nominal plant and the virtual control signal to mitigate the uncertainties of actuator failures.

One advantage of this adaptive control allocation structure is the ease in solving certain problems associated with direct adaptive control, such as the self-cancellation phenomenon. To remedy this problem, adaptive allocation gains can be bounded into certain ranges with same signs (e.g., via parameter projection) so that the allocated control signals cannot go to opposite directions. Another advantage of the adaptive control allocation is the reduction of the controller complexity. For instance, let us consider a state feedback adaptive control design for an n-state system with m controls. The number of controller parameters to be updated is of the order $\mathcal{O}(m \times n)$. If the problem can be solved in the adaptive control allocation framework with all actuators in one group, then an adaptive state feedback controller can be designed and allocated by the adaptive allocation gains before feeding into the actuators. In this case the updated parameters is of

the order $\mathcal{O}(m+n)$. For example, if we try to stabilize a 5-state system with 3 controls, the total adaptive parameters using a direct adaptive controller would be 15. If we can group the control inputs together without changing the controllability of the system and use the adaptive control allocation method, the total adaptive parameters would be 8. The parameter reduction is more obvious if more control effectors can be grouped together. Another advantage of this approach is that the virtual control signal can be designed using a non-adaptive state feedback approach, and the failure compensation is achieved by only adapting the control allocation gains. It implies that the proposed adaptive control allocation structure can be added to a conventionally designed state feedback control loop for improved reliability.

In this paper, we will illustrate the development of this adaptive control allocation design in detail. For the current research, we will concentrate on the adaptive control allocation for a single group of actuators. Two stable adaptive control allocation algorithms will be presented for both loss of effectiveness and constant-magnitude actuator failures. Technical issues such as design conditions, adaptive law designs, and stability analysis will be addressed in detail. The proposed schemes are shown to guarantee stability and asymptotic state tracking in the presence of unknown failures. Simulation studies of the proposed control allocation algorithms applied to aircraft control applications are performed, and simulation results are presented.

The paper is organized as follows. In Section II, we introduce the development of the adaptive control allocation algorithm for loss of effectiveness failures. A simulation study of the proposed algorithm applied to an aircraft lateral control problem is included. The adaptive control allocation scheme for constant actuator failure compensation illustrated in Section III. The proposed scheme is applied to control the pitch motion of a linearized transport aircraft model in the presence of constant-magnitude elevator failure, and simulation results are presented.

II. Adaptive Control Allocation Design for Loss of Effectiveness Failures

In this section, we will illustrate the design of adaptive control allocation algorithm for loss of effectiveness actuator failures. A simulation study will be presented with the proposed algorithm applied to the lateral control of a linearized transport aircraft model. The current study focuses on the adaptive control allocation for a single group of actuators, but the proposed algorithm can be extended to adaptive control allocation with multiple groups of actuators.

A. Problem Formulation

Plant description. In this study, we consider a linear time-invariant system in the following form

$$\dot{x}(t) = Ax(t) + Bu(t) \tag{1}$$

where $x \in R^n$ and $u \in R^m$ are the system state and the control input. The matrices $A \in R^{n\times n}$ and $B \in R^{n\times m}$ are constant. The matrix B is the control gain matrix for the group of actuators and it is assumed to be known for the adaptive control design.

The control signal $u(t)$ can be expressed as

$$u(t) = \Lambda v(t) \tag{2}$$

where $v(t)$ is the allocated control signals as actuator inputs and Λ is a piecewise constant uncertain diagonal control effectiveness matrix with $\Lambda = \text{diag}\{\lambda_1, \lambda_2, \ldots, \lambda_m\}$, and $0 < \lambda_i \leq 1$, $i = 1, \ldots, m$. The ith actuator is healthy if $\lambda_i = 1$ and has a loss of effectiveness failure if $0 < \lambda_i < 1$. For the design in this section, we assume that $\lambda_i \neq 0$, i.e., no actuator outage occurs. Thus Λ is always positive definite.

As mentioned earlier, the control input $v(t) = [v_1(t), v_2(t), \ldots, v_m(t)]^T$ contains the distributed control signals from a virtual control signal, i.e., v_j, $j = 1, \ldots, m$, can be denoted as

$$v_j(t) = \alpha_j(t) v_0(t), \qquad j = 1, 2, \ldots, m \tag{3}$$

where $v_0(t)$ is a control signal designed for the whole group, and $\alpha_j(t)$ is the adaptive allocation gain for jth actuator. We assume that the ideal allocation gains are known when there is no failure in the system. The *ideal allocation gain* vector is denoted as $\alpha^* \in R^m$. We also define the *equivalent control gain vector* as $b_0 \triangleq B\alpha^*$. The vector b_0 can be seen as the equivalent control gain matrix for the equivalent control effector representing the actuator group. For this study, we assume that the pair (A, b_0) is stabilizable.

Reference model. For the adaptive control, the desired closed-loop dynamics is designed as

$$\dot{x}_m(t) = A_m x_m(t) + B_m r(t) \tag{4}$$

where $A_m \in R^{n\times n}$ is a Hurwitz matrix, and $B_m \in R^n$. The signal $r(t) \in R$ is a bounded piecewise continuous reference input, and $x_m(t)$ is the desired state. For a given symmetric positive definite matrix $Q \in R^{n\times n}$, there exists a unique $P \in R^{n\times n}$ that satisfies

$$PA_m + A_m^T P = -Q, \text{ and } P = P^T > 0. \tag{5}$$

For the adaptive control design, we need the following standard plant model matching condition:

Assumption 1 *There exist constant $K_1^* \in R^n$, $K_2^* \in R$ such that the following equations are satisfied:*

$$A + b_0 K_1^{*T} = A_m, \qquad b_0 K_2^* = B_m. \tag{6}$$

In the above assumption, b_0 is the equivalent control gain matrix for the entire group of actuators.

Control objective. The control objective is to design the virtual control signal $v_0(t)$ and adaptive allocation gains α_j, $j = 1, \ldots, m$, such that all the closed-loop signals are bounded and the system state $x(t)$ tracks the desired state $x_m(t)$ asymptotically in the presence of uncertain loss of effectiveness failures characterized by Λ.

B. Adaptive Control Allocation Design

Nominal controller. The plant model matching condition in Assumption 1 indicates the existence of a nominal controller $v^*(t)$ for the system without failures and an ideal constant allocation gain vector α^* such that the closed-loop response is identical to that of the reference model when the responses of any unmatched initial conditions vanish exponentially. Such a nominal control signal has the following form

$$v_0^*(t) = K_1^{*T} x(t) + K_2^* r(t) \triangleq \theta^{*T} \omega(t), \qquad v^*(t) = \alpha^* v_0^*(t) \tag{7}$$

where $\theta^* \triangleq [K_1^{*T}, K_2^*]^T \in R^{n+1}$, and $\omega(t) = [x^T(t), r(t)]^T$. The above state feedback control $v_0^*(t)$ together with a pre-specified distribution α^* ensures the state tracking error $e(t) = x(t) - x_m(t)$ approaches zero exponentially.

Adaptive controller. When a failure occurs, the allocation gain α^* needs to be changed to accommodate the failure, but the new desired α^* may not be known due to the uncertainty of the failure. For accommodation of the uncertainty, we shall use the adaptive versions of control signal and allocation gain

$$v_0(t) = K_1^T(t) x(t) + K_2(t) r(t) = \theta^T(t) \omega(t), \qquad v(t) = \alpha(t) v_0(t) \tag{8}$$

where $K_1(t)$ and $K_2(t)$ are the estimates of K_1^* and K_2^*, and $\theta(t) = [K_1^T(t), K_2(t)]^T \in R^{n+1}$. The updated $\alpha(t) = [\alpha_1(t), \ldots, \alpha_m(t)]^T$ is the estimate of α^*. We also define the parameter errors as $\tilde{\theta}(t) = \theta(t) - \theta^*$.

Error dynamics. With the plant and control in (1) and (2), nominal controller in (7), and adaptive controller in (8), the closed-loop dynamics can be expressed as

$$\begin{aligned}
\dot{x}(t) &= Ax(t) + B\Lambda\alpha(t) v_0(t) \\
&= Ax(t) + B\alpha^* v_0(t) + B\tilde{\alpha}(t) v_0(t) \\
&= Ax(t) + b_0 v_0(t) + B\tilde{\alpha}(t) v_0(t) \\
&= Ax(t) + b_0 v_0^*(t) + b_0 \tilde{\theta}^T(t) \omega(t) + B\tilde{\alpha}(t) v_0(t) \\
&= (A + b_0 K_1^{*T}) x(t) + b_0 K_2^* r(t) + b_0 \tilde{\theta}^T(t) \omega(t) + B\tilde{\alpha}(t) v_0(t) \\
&= A_m x(t) + B_m r(t) + b_0 \tilde{\theta}^T(t) \omega(t) + B\tilde{\alpha}(t) v_0(t)
\end{aligned} \tag{9}$$

where $\tilde{\alpha}(t) \triangleq \Lambda\alpha(t) - \alpha^*(t)$.

From the closed-loop dynamics in (9) and reference model in (4), the error dynamics can be obtained as

$$\dot{e}(t) = A_m e(t) + b_0 \tilde{\theta}^T(t) \omega(t) + B\tilde{\alpha}(t) v_0(t). \tag{10}$$

It can be seen that the error dynamics in (10) is suitable for adaptive law design in that the latter half of its right hand side is linear in terms of the uncertain parameter error signals $\tilde{\theta}(t)$ and $\tilde{\alpha}(t)$.

Adaptive laws. Based on the error dynamics in (10), we can design the adaptive laws for the control parameter $\theta(t)$ and allocation gain $\alpha(t)$ as

$$\dot{\theta}(t) = -\Gamma_\theta \omega(t) e^T(t) P b_0, \tag{11}$$

$$\dot{\alpha}(t) = -\Gamma_\alpha B^T P e(t) v_0(t), \tag{12}$$

where Γ_θ and Γ_α are symmetric positive definite matrices and P is determined by (5). From the adaptive laws, we can see that the controller parameters of the virtual control signal for the actuator group are updated using the information of the equivalent control gain vector b_0. The allocation gains are updated with the B matrix since successful allocation of the virtual control signal to each actuator requires the knowledge of each column of B.

The properties of the adaptive control allocation scheme can be summarized in the following theorem.

Theorem 1 *For the system in (1), the adaptive controller and allocation scheme in (8), and the adaptive laws in (11) and (12) guarantee that the all the closed-loop signals are bounded and* $\lim_{t\to\infty}[x(t) - x_m(t)] = 0$ *in the presence of uncertain loss of effectiveness actuator failures in (2).*

Proof. When a failure occurs, the control effectiveness matrix Λ has a discontinuity. It would lead to a finite jump in $\tilde{\alpha}(t)$ as well, which could result in a a finite jump in the error dynamics. Let us assume that there are l failures occurring in the system, and the actuator failures occur at time instants t_k, with $t_k < t_{k+1}$, $k = 1, 2, \ldots, N$. For the closed-loop stability and state tracking analysis, we choose the following Lyapunov-like function

$$V(t) = \frac{1}{2} e^T(t) P e(t) + \frac{1}{2} \tilde{\alpha}^T(t) \Gamma_\alpha^{-1} \Lambda^{-1} \tilde{\alpha}(t) + \frac{1}{2} \tilde{\theta}^T(t) \Gamma_\theta^{-1} \tilde{\theta}(t) \tag{13}$$

for each time interval (t_k, t_{k+1}), $k = 0, 1, \ldots, N$ with $t_0 = 0$ and $t_{N+1} = \infty$. $V(t)$ is thus discontinuous with finite jumps at t_k, $k = 1, \ldots, N$. Taking the time derivative of $V(t)$ and substituting the adaptive laws in (11) and (12) into the result for each (t_k, t_{k+1}), we obtain

$$\begin{aligned} \dot{V}(t) &= e^T(t) P \dot{e}(t) + \tilde{\alpha}^T(t) \Gamma_\alpha^{-1} \dot{\alpha}(t) + \tilde{\theta}^T(t) \Gamma_\theta^{-1} \dot{\theta}(t) \\ &= e^T(t) P [A_m e(t) + b_0 \tilde{\theta}^T(t) \omega(t) + B \tilde{\alpha}(t) v_0(t)] - \tilde{\alpha}^T(t) B^T P e(t) v_0(t) - \tilde{\theta}^T(t) \omega(t) e^T(t) P b_0 \\ &= -\frac{1}{2} e^T Q e \leq 0. \end{aligned} \tag{14}$$

Thus we can conclude that for each (t_k, t_{k+1}), $k = 0, 1, \ldots, N$, $V(t)$ is bounded. Since $V(t)$ only has finite jumps at t_k, $k = 1, \ldots, N$, we can conclude that $V(t)$ is bounded for $t \in [0, \infty)$, and $e(t) \in L^\infty$, $\tilde{\alpha}(t) \in L^\infty$, $\tilde{\theta}(t) \in L^\infty$, $\alpha(t) \in L^\infty$, $\theta(t) \in L^\infty$, $x(t) \in L^\infty$, and $\omega(t) \in L^\infty$. Integrating both sides of (14), we can obtain

$$V(t_k^+) - V(t_{k+1}^-) = \frac{1}{2} \int_{t_k}^{t_{k+1}} e^T(\tau) Q(\tau) e(\tau) d\tau. \tag{15}$$

For $N + 1$ intervals: $[0, t_1)$, (t_1, t_2), ..., (t_{N-1}, t_N), and (t_N, ∞), (15) holds. Summing both sides of (15) for $k = 0, 1, \ldots, N$, we can have

$$\begin{aligned} \frac{1}{2} \int_0^\infty e^T(\tau) Q(\tau) e(\tau) d\tau &= V(0) - V(t_1^-) + V(t_1^+) - V(t_2^-) + V(t_2^+) - \cdots - V(t_k^-) + V(t_k^+) \\ &\quad - \cdots - V(t_N^-) + V(t_N^+) - V(\infty) \\ &= V(0) + \sum_{i=1}^{N} [V(t_i^+) - V(t_i^-)] - V(\infty) < \infty \end{aligned} \tag{16}$$

because the jumps $V(t_i^+) - V(t_i^-)$ are finite and the number N of jumps is also finite. Thus we have $e(t) \in L^2$. We can also conclude from (10) that $\dot{e}(t) \in L^\infty$. So from $e(t) \in L^2 \cap L^\infty$, and $\dot{e}(t) \in L^\infty$, we have $\lim_{0\to\infty} e(t) = 0$. □

C. Simulation Study

In this simulation study, the application of the proposed adaptive control allocation scheme to a linearized transport aircraft model is demonstrated. The proposed scheme will be applied to control the aircraft to make a turn. Two simulation cases will be discussed and the simulation results will be presented in detail.

Model description. For this simulation study, the linearized lateral dynamic model of a large transport aircraft flying in a steady wings-level cruise condition[13] is used. The aircraft model is

$$\dot{x} = Ax + Bu, \tag{17}$$

$$x = [v_b, p_b, r_b, \phi, \psi]^T, \tag{18}$$

$$u = [\delta_a, \delta_r]^T. \tag{19}$$

The state includes the lateral velocity v_b (ft/s), roll rate p_b (rad/s), yaw rate r_b (rad/s) (all in body-axis frame), roll angle ϕ (rad) and yaw angle ψ (rad). The control inputs are aileron δ_a and rudder δ_r deflections (deg). The system matrices A and B are

$$A = \begin{bmatrix} -0.129 & 28.328 & -774.92 & 32.145 & 0 \\ -0.012 & -1.4419 & 0.9409 & 0 & 0 \\ 0.004 & -0.0409 & -0.1757 & -0.0001 & 0 \\ 0 & 1 & 0.0372 & 0 & 0 \\ 0 & 0 & 1.0007 & 0 & 0 \end{bmatrix}, \quad B = \begin{bmatrix} 0.0542 & 0.4669 \\ 0.0443 & 0.0200 \\ 0.0025 & -0.0382 \\ 0 & 0 \\ 0 & 0 \end{bmatrix}. \tag{20}$$

In this simulation study, we will include the aileron and rudder into one group, for which a control signal will be designed and allocated. This example shows that the grouped control surfaces are not necessarily of the same physical functionality type. They can be grouped as long as they can work in a coordinated fashion. Aileron and rudder of an aircraft are usually used in a coordinated fashion in lateral maneuvers, thus we include them in one group in this simulation.

An important outcome of the grouping is the reduction of the computational complexity. If adaptive control signals are designed separately for the two control inputs with the state feedback structure, the total updated parameters would be $(5+1)\times 2 = 12$. They include 5 state feedback parameters and 1 feed-forward parameter (for tracking the reference input) for each control surface. The adaptive control allocation scheme, on the other hand, requires $5 + 1 + 2 = 8$ parameters since only one adaptive control signal is designed and allocated with two updated allocation gains.

Nominal parameters. The ideal allocation gain vector is selected as $\alpha^* = [8.6103, -1]^T$, thus the equivalent control gain vector is $b_0 = B\alpha^* = [0, 0.3614, 0.0594, 0, 0]^T$. The ideal allocation gain is chosen so that the first element in b_0, i.e., the control gain for the lateral acceleration, is zero. The purpose of this choice is to minimize the side slip when aircraft is turning.

The nominal controller is designed based on the LQR approach for (A, b_0). The resulting gains are

$$K_1^* = [-0.8963, 22.1655, -73.6645, 28.8488, 4.0825]^T, \qquad K_2^* = 1. \tag{21}$$

Reference model. For this simulation study, the reference model is chosen as the closed-loop dynamics with the above LQR controller, i.e.,

$$A_m = A + b_0 K_1^*, \qquad B_m = b_0 K_2^*. \tag{22}$$

The reference input to the reference model is chosen as $r(t) = 2.1376$ for $t \geq 0$, which leads to a desired state trajectory with steady-state values

$$x_m(\infty) = [0, 0, 0, 0, 0.5236]^T. \tag{23}$$

Its physical meaning is that the aircraft turns to right with its yaw angle increased by 0.5236 rad (30 deg).

Actuator failure. The actuator failure considered in this simulation is a loss of effectiveness failure of the aileron deflection. The aileron maintains only 20% of its effectiveness after 10 seconds, i.e.,

$$u_1(t) = 0.2v_1(t), \quad \text{for } t \geq 10 \text{ seconds} \tag{24}$$

where $u_1(t)$ is the output of the aileron actuator and $v_1(t)$ is the designed control input to aileron.

Simulation results. The results of two simulation cases will be presented in this paper:

- Case I: adaptive allocation of the adaptive control signal designed in Section II.B (Eqs. (11) and (12)).
- Case II: adaptive allocation (as in Eq. (12)) of the non-adaptive control signal with fixed gains as in Eq. (21).

For a clear presentation of the simulation results, the units of angles and angular velocities in the state $x(t)$ are converted from (rad) and (rad/s) to (deg) and (deg/s), respectively, in the plots hereafter.

Case I. In this case, we apply the proposed adaptive control allocation in Section II.B to the aircraft model. The adaptive state feedback control signal is designed and adaptively allocated to both aileron and rudder. The controller parameters start from 80% of their nominal values in Eq. (21). The time history of the system state under failure and the desired state is shown in Figure 2. It can be seen that the asymptotic state tracking is achieved after the failure occurs at 10 seconds.

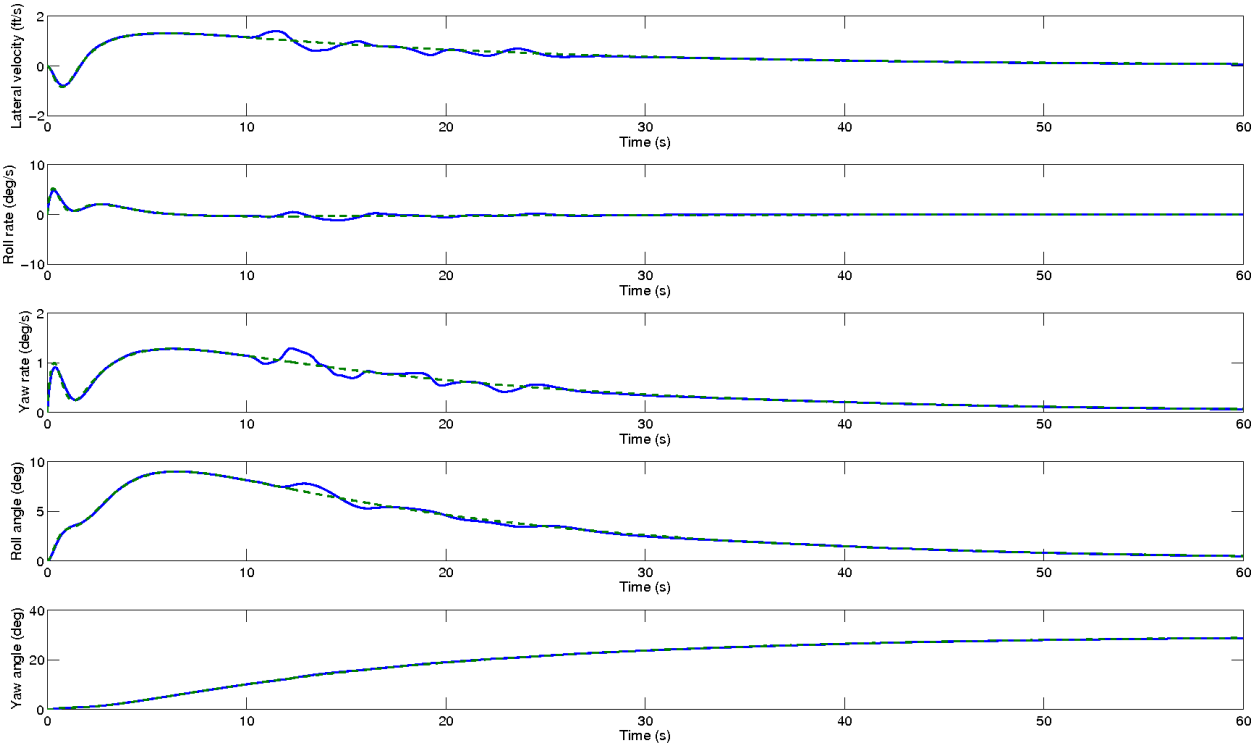

Figure 2. Time history of plant state (solid) and reference model state (dashed) (Case I).

Figure 3 shows the designed control signal $v_0(t)$, allocated control signals $v(t)$ and actuator outputs $u(t)$. The designed control signal is allocated by the adaptive allocation gains.The actuator outputs are different from the allocated control signals since there is an actuator failure.

The adaptation of the controller parameters is shown in Figure 4. We can see that $K_2(t)$ also plays an important role in the compensation of actuator failures. The adaptive allocation gains are shown in Figure 5. The two allocations gains adapt immediately after the failure occurs, and settle to a new combination of steady-state values that, together with $K_2(t)$ and $K_1(t)$, guarantee the state tracking after failure.

Case II. In this simulation case, we apply the adaptive allocation scheme with the LQR nominal controller with K_1^* and K_2^* in (21). The purpose of this example is to verify the failure compensation capability of the adaptive allocation gains without the adaptation of the controller parameters.

The system state and desired state are shown in Figure 6. Despite the uncertain actuator failure, the asymptotic state tracking is eventually achieved. The designed control signal, allocated control signals and the actuator outputs are shown in Figure 7. Similar to the previous case, the allocated control signals and the actuator outputs are not identical due to the actuator failure. The allocation gains are shown in Figure 8. The allocation gains are updated autonomously for failure compensation.

In this simulation case, we have achieved similar results to Case I with a slightly degraded transient response. A possible explanation for it is that the controller parameters are fixed in this case and cannot

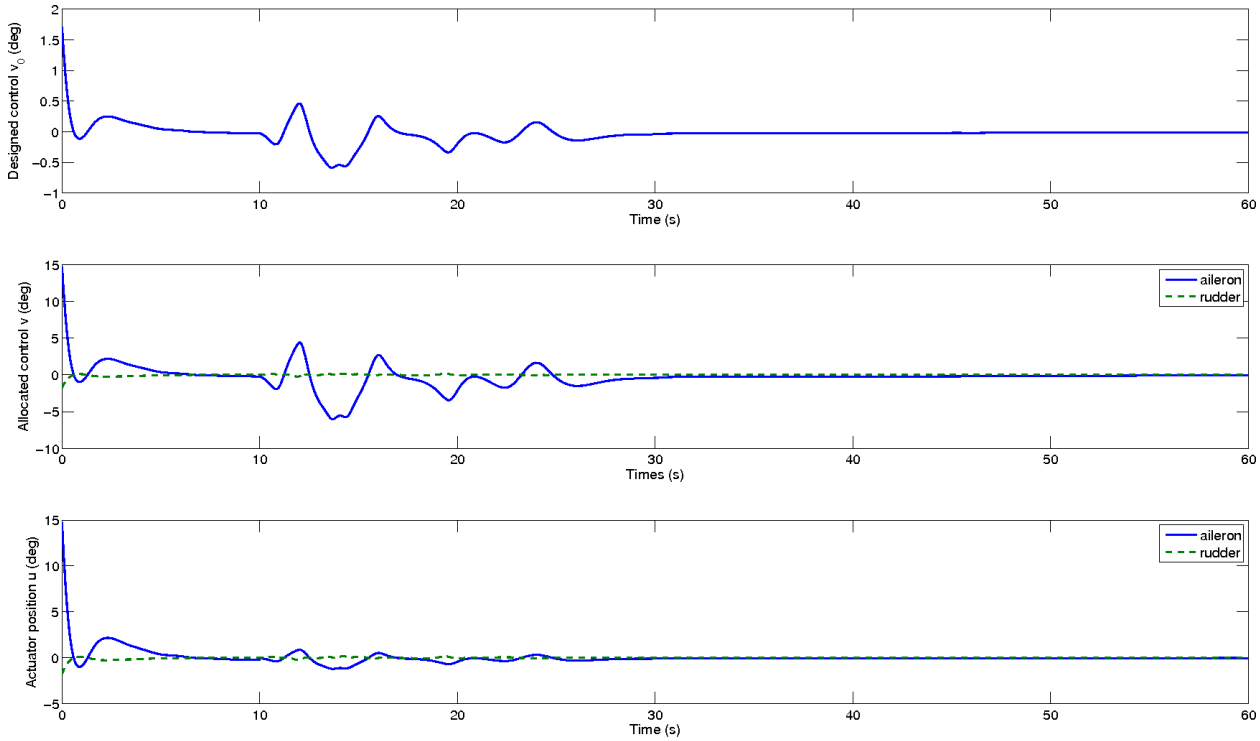

Figure 3. Time history of control signals and actuator outputs (Case I).

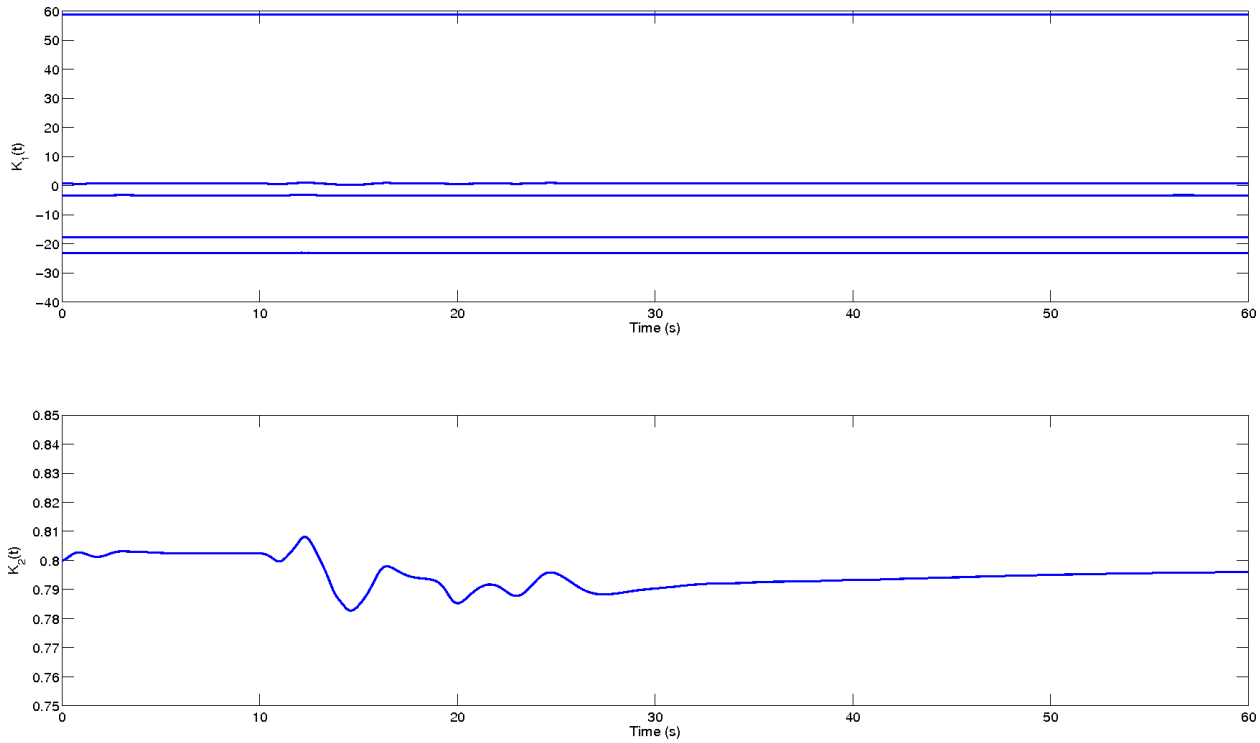

Figure 4. Time history of controller parameters (Case I).

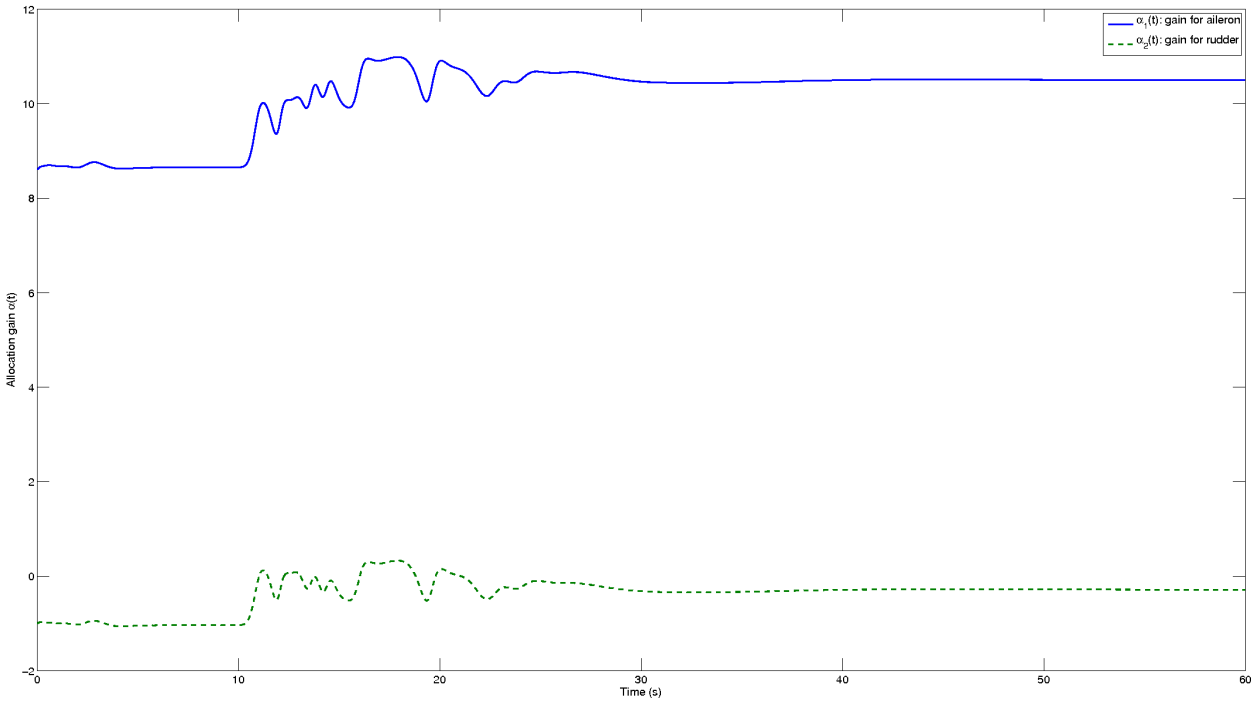

Figure 5. Time history of allocation gains (Case I).

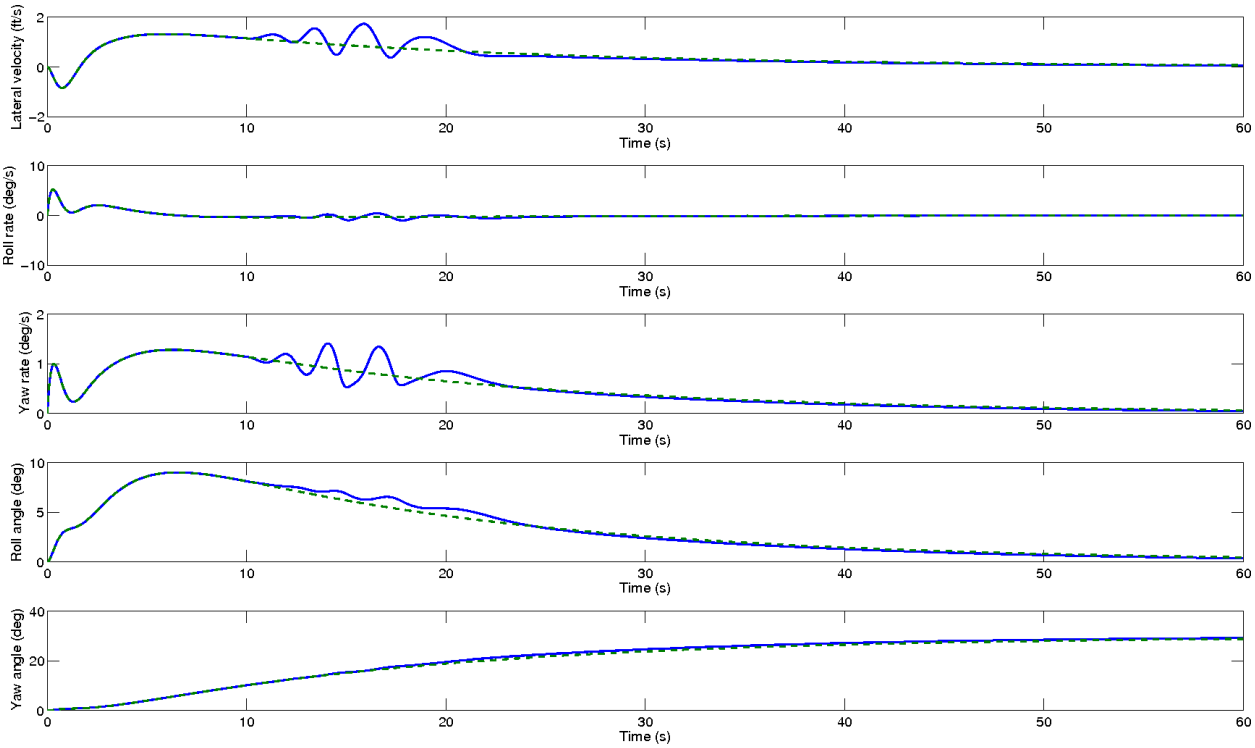

Figure 6. Time history of plant state (solid) and reference model state (dashed) (Case II).

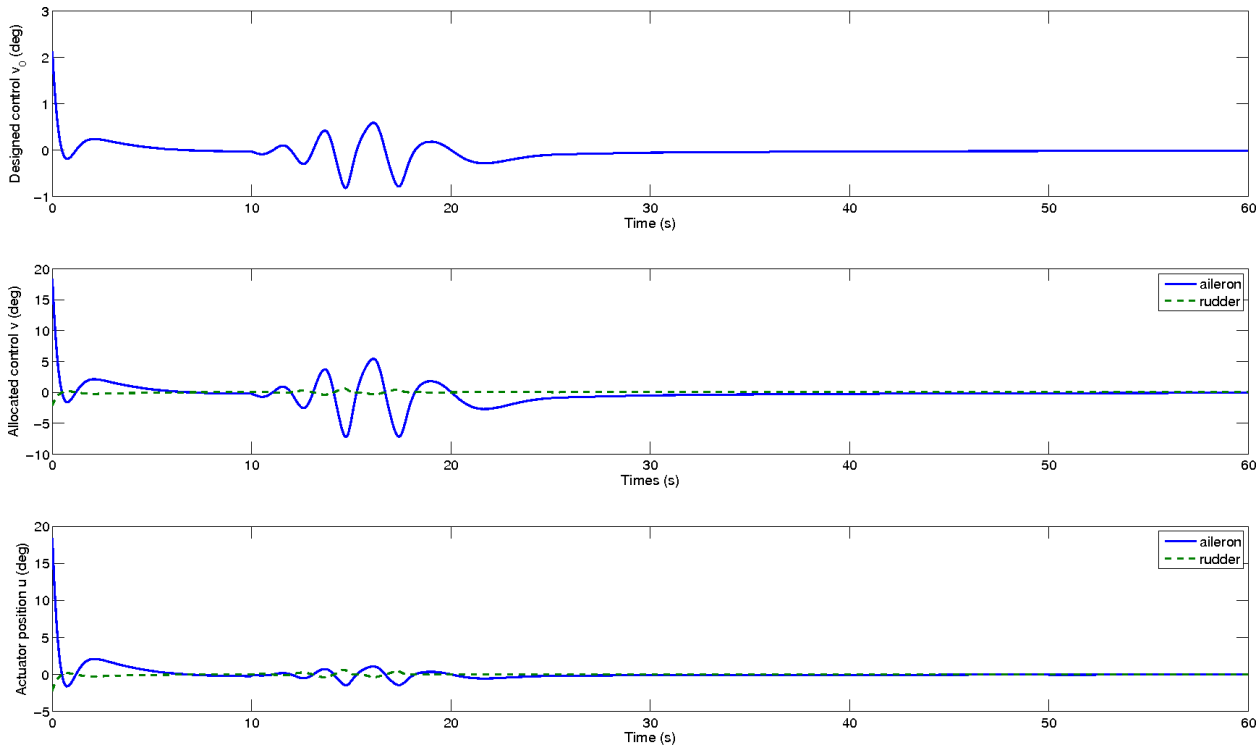

Figure 7. Time history of control signals and actuator outputs (Case II).

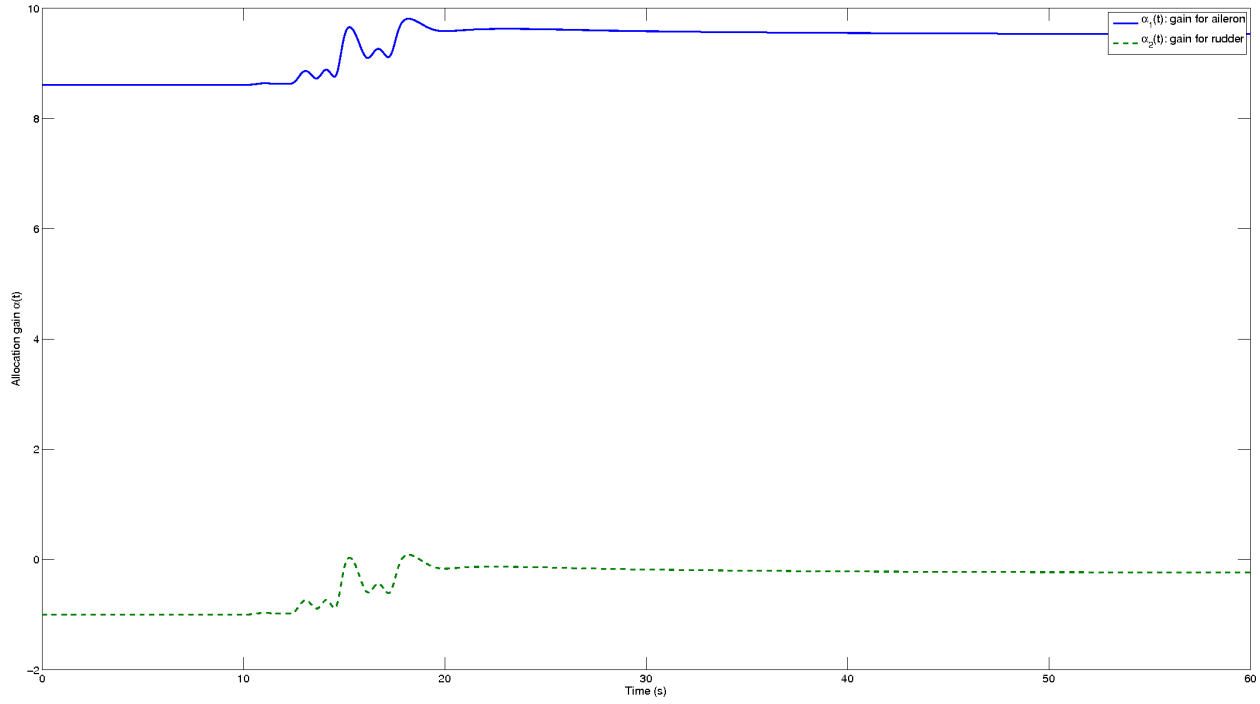

Figure 8. Time history of allocation gains (Case II).

contribute to the failure compensation and trajectory tracking as they do in Case I. However, the closed-loop stability and asymptotic state tracking are guaranteed even though only the allocation gains are adapted. The successful demonstration of failure compensation in Case II implies that the proposed adaptive allocation unit can be added to a control loop with a conventional state feedback controller. The added adaptive allocation to the non-adaptive controller ensures the closed-loop stability and asymptotic state tracking despite uncertain actuator failures.

III. Adaptive Control Allocation Design for Constant Failures

In this section, we develop an adaptive control allocation scheme for the compensation of constant-magnitude actuator failures. A redundancy condition required for this design will be introduced, and the controller structure, adaptive law design, and stability analysis will be discussed.

A. Problem Formulation

When constant failures are present in the system, the control signal can be rewritten as[10]

$$u(t) = v(t) + \sigma_f(\bar{u} - v(t)) \tag{25}$$

where $\bar{u} = [\bar{u}_1, \ldots, \bar{u}_m]^T$ is the failure vector whose elements are unknown constants, and σ_f represents the failure pattern and is defined as

$$\sigma_f = \text{diag}\{\sigma_1, \sigma_2, \ldots, \sigma_m\} \tag{26}$$

with $\sigma_i = 1$ if the ith actuator has failed, that is, $u_i = \bar{u}_i$, and $\sigma_i = 0$ otherwise. The failures are assumed to occur instantaneously, i.e., σ_i are piecewise constant.

The plant dynamics can then be rewritten as

$$\dot{x}(t) = Ax(t) + B(I - \sigma_f)v(t) + B\sigma_f\bar{u}. \tag{27}$$

The constant failure $\bar{u}$ introduces an uncertain disturbance that needs to be accommodated. The control objectives for this adaptive control allocation scheme is to design $v(t)$ to guarantee the closed-loop stability and asymptotic state tracking when uncertain constant failures occur.

For adaptive control of constant actuator failures, sufficient built-in actuation redundancy is required. The redundancy condition is described in the following assumption:

Assumption 2 *The rank of B matrix satisfies that* $\text{rank}[B] = 1$*, and there is at least one operable actuator in the system.*

The rank condition characterizes the redundancy of actuation which is necessary for a successful constant failure compensation. Based on this condition, there can be up to $m - 1$ constant actuator failures. This condition can be satisfied for practical systems, such as the NASA Generic Transport Model (GTM)[14,15] which uses an elevator that consists of four segments. A longitudinal dynamic model linearized from NASA GTM is presented in Section III.C and it can be seen that the B matrix in this model has rank 1.

Similar to Section II, the design in this section consists of a nominal controller for the system without any uncertainties.

Nominal controller. For failure compensation purpose, we consider the following nominal controller structure

$$v_0^*(t) = K_1^{*T}x(t) + K_2^*r(t) + K_3^* \triangleq \bar{\theta}^{*T}\bar{\omega}(t), \qquad v^*(t) = \alpha^* v_0^*(t) \tag{28}$$

where $\bar{\theta}^* = [K_1^{*T}, K_2^*, K_3^*]^T$ and $\bar{\omega} = [x^T(t), r(t), 1]^T$. When there is no failure in the system, K_1^*, K_2^* and α^* can be chosen as in (6), and K_3^* can be set to be zero. In this way, the controller ensures the match between the reference model and the nominal plant without failures. Similar to the previous subsection, we also define $B\alpha^* = b_0$ which is known for the controller design.

Next we will show that the controller in (28) can guarantee the plant model matching if failures do occur. When there are failures in the system, K_3^* cannot generally be zero, and a new set of allocation gains, denoted $\bar{\alpha}^*$, may be needed, which may not necessarily equal the original allocation gains α^*. From (27) and (28) we may obtain

$$\dot{x} = Ax + B(I - \sigma_f)\bar{\alpha}^*(K_1^{*T}x + K_2^*r + K_3^*) + B\sigma_f\bar{u}. \tag{29}$$

We assume that at most p actuators can fail with $p \leq m-1$. Define an index set for failed actuators as $F = \{i_1, \ldots, i_p\}$ such that $\sigma_k = 1$ for any $k \in F$. Then $B(I-\sigma_f)\bar{\alpha}^*$ can be expressed as

$$B(I-\sigma_f)\bar{\alpha}^* = \sum_{j \notin F} b_j \bar{\alpha}_j^* \tag{30}$$

where b_j is the jth column of B and $\bar{\alpha}_j^*$ is the jth element of $\bar{\alpha}^*$.

Based on the rank condition in Assumption 2, we know that all columns of B are parallel, i.e., for any two columns of B, b_i and b_j, $b_i = c_{ij} b_j$ where c_{ij} is a constant scalar. Thus we know that the vector $b_0 = B\alpha^*$, which is the linear combination of all columns of B, is also parallel to any column in B. So for each column b_k in B, $k = 1, 2, \ldots, m$, we can find a constant nontrivial scalar c_k such that $b_k = c_k b_0$. Therefore (30) can be further expressed as

$$B(I-\sigma_f)\bar{\alpha}^* = \sum_{j \notin F} b_j \bar{\alpha}_j^* = \sum_{j \notin F} c_j \bar{\alpha}_j^* b_0. \tag{31}$$

If $\bar{\alpha}_j^*$, $j \notin F$ are chosen such that

$$\sum_{j \notin F} c_j \bar{\alpha}_j^* = 1, \tag{32}$$

then we may obtain

$$B(I-\sigma_f)\bar{\alpha}^* = b_0. \tag{33}$$

One possible choice for $\bar{\alpha}_j^*$, $j \notin F$ is

$$\bar{\alpha}_j^* = \frac{1}{c_j(m-p)} \tag{34}$$

Equation (33) indicates that, under constant failures, the plant model condition in (6) can still be satisfied. Note that for the system without failures

$$B\alpha^* = \sum_{j=1}^{m} \alpha_j^* b_j = \sum_{j=1}^{m} c_j \alpha_j^* b_0 = b_0 \tag{35}$$

which implies that

$$\sum_{j=1}^{m} c_j \alpha_j^* = 1. \tag{36}$$

Comparing (32) and (36), we can see that $\bar{\alpha}^*$ is generally different from α^*.

For $B\sigma_f \bar{u}$, we can also get

$$B\sigma_f \bar{u} = \sum_{k \in F} b_k \bar{u}_k = \sum_{k \in F} c_k \bar{u}_k b_0 \triangleq d^* b_0. \tag{37}$$

With (33) and (37), (29) can be expressed as

$$\dot{x}(t) = Ax(t) + b_0 K_1^{*T} x(t) + b_0 K_2^* r(t) + b_0 K_3^* + d^* b_0. \tag{38}$$

By choosing $K_3^* = -d^*$, we have $b_0 K_3^* = -B\sigma_f \bar{u}$, and (38) can be reduced to

$$\dot{x}(t) = Ax(t) + b_0 K_1^{*T} x(t) + b_0 K_2^* r(t) = (A + b_0 K_1^{*T}) x(t) + b_0 K_2^* r(t). \tag{39}$$

Therefore when failures are present, a nominal controller can always be found, with K_1^* and K_2^* specified in (6), $\bar{\alpha}^*$ characterized in (32), and $K_3^* = -d^*$ ensures that the closed-loop system is stable under failures, and the state converges to the desired state x_m in (4) exponentially.

B. Adaptive Control Allocation Design

Adaptive controller. Due to the uncertain nature of the failures, the desired controller parameters under failures are unknown. Thus we need the following adaptive control allocation scheme.

$$v_0(t) = K_1^T(t)x(t) + K_2(t)r(t) + K_3(t) \triangleq \bar{\theta}^T(t)\bar{\omega}(t), \qquad v(t) = \alpha(t)v_0(t), \tag{40}$$

where $K_1(t)$, $K_2(t)$, and $K_3(t)$ are the estimates of K_1^*, K_2^*, and K_3^* in (28). The signal $\bar{\omega}(t) = [x^T(t), r(t), 1]^T$. With the adaptive controller in (40) and the plant dynamics in (27), the closed-loop system dynamics can be obtained as

$$\dot{x}(t) = Ax(t) + B(I - \sigma_f)\alpha(t)[K_1^T(t)x(t) + K_2(t)r(t) + K_3(t)] + B\sigma_f\bar{u}. \tag{41}$$

Error dynamics. For this adaptive control scheme design, we redefine $\tilde{\alpha}(t) \triangleq \alpha(t) - \bar{\alpha}^*$, and (41) becomes

$$\begin{aligned}
\dot{x}(t) &= Ax(t) + B(I - \sigma_f)\alpha(t)v_0(t) + B\sigma_f\bar{u} \\
&= Ax(t) + B(I - \sigma_f)\tilde{\alpha}(t)v_0(t) + B(I - \sigma_f)\bar{\alpha}^*v_0(t) + B\sigma_f\bar{u} \\
&= Ax(t) + B(I - \sigma_f)\tilde{\alpha}(t)v_0(t) + B(I - \sigma_f)\bar{\alpha}^*v_0^*(t) + B(I - \sigma_f)\bar{\alpha}^*\tilde{v}_0(t) + B\sigma_f\bar{u}
\end{aligned} \tag{42}$$

where $\tilde{v}_0(t) = (\bar{\theta}(t) - \bar{\theta}^*)^T\bar{\omega}(t) \triangleq \tilde{\theta}^T(t)\bar{\omega}(t)$.

With (33), $B(I - \sigma_f)\bar{\alpha}^*v_0^*(t)$ in (42) becomes

$$B(I - \sigma_f)\bar{\alpha}^*v_0^*(t) = b_0v_0^*(t) = b_0K_1^{*T}x(t) + b_0K_2^*r(t) + b_0K_3^*. \tag{43}$$

With (43), (42), and the plant model matching condition in (6), we have

$$\dot{x}(t) = A_mx(t) + B_mr(t) + B(I - \sigma_f)\tilde{\alpha}(t)v_0(t) + b_0\tilde{\theta}^T(t)\bar{\omega}(t). \tag{44}$$

From the closed-loop dynamics in(44) and the reference model in (4), we can obtain the error dynamics

$$\dot{e}(t) = A_me(t) + B(I - \sigma_f)\tilde{\alpha}(t)v_0(t) + b_0\tilde{\theta}^T(t)\bar{\omega}(t). \tag{45}$$

Adaptive laws. From the error dynamics in (45), the following adaptive laws can be designed for the adaptive parameters:

$$\dot{\bar{\theta}}(t) = -\Gamma_\theta\bar{\omega}(t)e^T(t)Pb_0, \tag{46}$$

$$\dot{\alpha}_j(t) = -\gamma_je^T(t)Pb_jv_0(t), \qquad j = 1, 2, \ldots, m, \tag{47}$$

where b_j is the jth column of B, $\gamma_j > 0$ and $\Gamma_\theta = \Gamma_\theta^T > 0$ are adaptive gains.

The following theorem summarizes the properties of the adaptive control allocation scheme:

Theorem 2 *The adaptive control allocation scheme in (40) with the adaptive laws in (46) and (47) applied to the plant in (27) in the presence of constant failures guarantees that all closed-loop signals are bounded and* $\lim_{t\to\infty}(x(t) - x_m(t)) = 0$.

Proof. In Section III.A, we have assumed that there are at most $p \leq m - 1$ constant actuator failures and defined an index set for failed actuators as $F = \{i_1, \ldots, i_p\}$ such that $\sigma_k = 1$ for all $k \in F$. Here we further assume that the failures occur at instants t_k, with $t_k < t_{k+1}$, $k = 1, 2, \ldots, N$ with $1 \leq N \leq p$. The number of failure instants may be smaller than the total number of failures since multiple failures may happen at the same time. For the stability proof, we choose the following Lyapunov-like function

$$V(t) = \frac{1}{2}e^T(t)Pe(t) + \frac{1}{2}\sum_{i\notin F}\gamma_i^{-1}\tilde{\alpha}_i^2(t) + \frac{1}{2}\tilde{\theta}^T(t)\Gamma_\theta^{-1}\tilde{\theta}(t) \tag{48}$$

for each time interval (t_k, t_{k+1}), $k = 0, 1, \ldots, N$, with $t_0 = 0$ and $t_{N+1} = \infty$. The time derivative in each time interval (t_k, t_{k+1}) is

$$\begin{aligned}
\dot{V}(t) &= e^T(t)P\dot{e}(t) + \sum_{i\notin F}\gamma_i^{-1}\tilde{\alpha}_i(t)\dot{\alpha}_i(t) + \tilde{\theta}^T(t)\Gamma_\theta^{-1}\dot{\bar{\theta}}(t) \\
&= e(t)^TPA_me(t) + e^T(t)PB(I - \sigma_f)\tilde{\alpha}(t)v_0(t) + e^T(t)Pb_0\tilde{\theta}^T(t)\bar{\omega}(t) \\
&\quad -e^T(t)Pv_0(t)\sum_{i\notin F}\tilde{\alpha}_i(t)b_i - \tilde{\theta}^T(t)\bar{\omega}(t)e^T(t)Pb_0 \\
&= e^T(t)PA_me(t) = -\frac{1}{2}e^T(t)Qe(t) \leq 0
\end{aligned} \tag{49}$$

with the fact that $B(I-\sigma_f)\tilde{\alpha}(t)=\sum_{i\notin F}\tilde{\alpha}_i(t)b_i$. Following a similar approach to the stability analysis in Section II, we can conclude that for any $t\in[0,\infty)$, $V(t)\in L^\infty$, $e(t)\in L^\infty$, $x(t)\in L^\infty$, $\bar{\omega}(t)\in L^\infty$, $\bar{\theta}(t)\in L^\infty$, $v_0(t)\in L^\infty$, $e(t)\in L^2$. Since $V(t)$ only includes $\tilde{\alpha}_i(t)$ with $i\notin F$, we can only conclude the boundedness of $\tilde{\alpha}_i(t)$ and $\alpha_i(t)$ for $i\notin F$. To show the boundedness of $\alpha_j(t)$, $j\in F$, we note that for any $j\in F$

$$\alpha_j(t)=\alpha_j(0)-\int_0^t\gamma_j e(\tau)^T P v_0(\tau)b_j d\tau, \tag{50}$$

based on the adaptive law in (47). Note that all the columns of B are parallel based on the rank condition in Assumption 2. So we can have

$$b_j=c_j^* b_k,\qquad \forall j\in F \tag{51}$$

where b_k is the column of B that corresponds to an arbitrary healthy actuator, i.e., $k\notin F$, and c_j^* is a non-zero constant. (50) can thus be expressed as

$$\begin{aligned}
\alpha_j(t) &= \alpha_j(0)-\int_0^t\gamma_j e(t)^T P v_0(t)c_j^* b_k dt\\
&= \alpha_j(0)-\frac{\gamma_j}{\gamma_k}c_j^*\int_0^t\gamma_k e(t)^T P v_0(t)b_k dt\\
&= \alpha_j(0)+\frac{\gamma_j}{\gamma_k}c_j^*\int_0^t(-\gamma_k e(t)^T P v_0(t)b_k)dt\\
&= \alpha_j(0)+\frac{\gamma_j}{\gamma_k}c_j^*\int_0^t\dot{\alpha}_k(t)dt\\
&= \alpha_j(0)+\frac{\gamma_j}{\gamma_k}c_j^*[\alpha_k(t)-\alpha_k(0)],\quad \forall j\in F.
\end{aligned} \tag{52}$$

Since $\alpha_k(t)$, $k\notin F$ has been proved to be bounded, we have $\alpha_j(t)\in L^\infty$, for $j\in F$.

We can further obtain that $\dot{e}(t)\in L^\infty$ from (45). With $e(t)\in L^\infty\cap L^2$ and $\dot{e}(t)\in L^\infty$, we can have $\lim_{t\to\infty}e(t)=0$. □

C. Simulation Study

In this subsection, we demonstrate the performance of the proposed adaptive control scheme in Section (III.B) with a longitudinal dynamic model linearized from the NASA Generic Transport Model.

Model description. The linearized aircraft model is of the following form.

$$\dot{x} = Ax+Bv, \tag{53}$$
$$x = [V_T,\alpha_a,q,\theta]^T, \tag{54}$$
$$v = [\delta_{elob},\delta_{elib},\delta_{erob},\delta_{erib}]^T \tag{55}$$

where the state includes the true airspeed (V_T) (ft/s), angle of attack (α_a) (rad), pitch rate q (rad/s), and pitch angle θ (rad). The control inputs are the deflections of the four elevator segments: left outboard elevator δ_{elob}, left inboard elevator δ_{elib}, right outboard elevator δ_{erob}, and right inboard elevator δ_{erib} (deg). The system matrices A and B are

$$A=\begin{bmatrix}-0.0450 & -8.9632 & 0.0349 & -32.1740\\ -0.0035 & -2.7429 & 0.9514 & 0\\ -0.0056 & -42.6233 & -3.5616 & 0\\ 0 & 0 & 1 & 0\end{bmatrix},\quad B=\begin{bmatrix}-0.0110 & -0.0110 & -0.0110 & -0.0110\\ -0.0012 & -0.0012 & -0.0012 & -0.0012\\ -0.1962 & -0.1962 & -0.1962 & -0.1962\\ 0 & 0 & 0 & 0\end{bmatrix} \tag{56}$$

It can be verified that $\text{rank}[B]=1$. For the simulation study, we will include the four elevator surfaces into one group, for which an elevator control signal will be designed and allocated.

Nominal parameters. The nominal allocation gain α^* is chosen as $\alpha^*=[1,1,1,1]^T$ and $b_0=B\alpha^*=[-0.0441,-0.0048,-0.7846,0]^T$. The nominal controller is designed based on the LQR approach for (A,b_0). The resulting gains are

$$K_1^*=[0.2619,19.8948,-6.3656,-18.9073],\qquad K_2^*=1. \tag{57}$$

Reference model. Similar to the simulation study in Section II, the reference model is chosen as the closed-loop dynamics of the LQR controller, i.e.,

$$A_m = A + b_0 K_1^*, \qquad B_m = b_0 K_2^*. \tag{58}$$

The reference input to the reference model is chosen as $r(t) = 3.2356$ for $t \geq 0$, which leads to a reference trajectory with steady-state values

$$x_m(\infty) \;=\; [10, -0.0139, 0, -0.0110]^T, \tag{59}$$

whose physical meaning is that the aircraft speed is increased by 10 ft/s; its angle of attack is reduced by 0.0139 rad (0.7964 deg); its pitch angle is reduced by 0.0110 rad (0.6303 deg).

Actuator failure. The actuator failure considered in this simulation is that the left outboard elevator is stuck at 10 degree after 1 second, i.e.,

$$u_1(t) = 10 \text{ deg }, \quad \text{ for } t \geq t_f \text{ second} \tag{60}$$

where $t_f = 1$ second. The signal $u_1(t)$ is the output of the left outboard elevator. It is stuck at $t_f = 1$ second and cannot respond to the elevator input $v_1(t)$.

Simulation results. For this simulation study, we present the results of two simulation cases.

In Case I, we will show the results of the adaptive control allocation of the adaptive control signal with the design in Section III.B. The adaptive control allocation scheme is expected to compensate for the uncertain actuator failure while maintaining stability and asymptotic tracking performance.

In Case II, we explore the performance of the proposed adaptive control allocation scheme with "pure" control allocation. Pure control allocation means that $\sum_{i=1}^{4} \alpha_i(t) = 1$, so that the adaptive allocation gains do not act as adaptive control parameters. To guarantee the above pure allocation condition in this case study, we update the first three adaptive gains, $\alpha_i(t)$, $i = 1, 2, 3$ using the adaptive laws in (47), and let the fourth one to be $\alpha_4(t) = 1 - \sum_{i=1}^{3} \alpha_i(t)$. Parameter projection is also applied to ensure that $\alpha_i(t)$, $i = 1, 2, 3$, are bounded within $(0, 0.25]$, so that all the adaptive allocation gains are positive and the elevator segments do not deflect in opposite directions. In this way, no mutual-cancellation would occur.

Case I. The simulation results for Case I are shown in Figures 9, 10, 11, and 12. The simulation results show that, despite the uncertain constant failure, the closed-loop signals in the system are all bounded and the state tracking error approaches zero asymptotically.

Case II. The simulation results of this case are shown in Figures 13, 14, 15, and 16. The closed-loop stability and asymptotic tracking can be guaranteed under the additional allocation constraints. It can be seen that the adaptive allocation gains act only for control allocation purpose and their function as adaptive control parameters is minimized.

IV. Conclusions

The adaptive control allocation problem has been studied in this paper and a novel adaptive control allocation framework has been proposed. The adaptive allocation scheme includes an adaptive control signal and a control allocation unit with adaptively updated allocation gains. Two adaptive control allocation algorithms have been proposed for the compensation of uncertain failures. The proposed algorithms have been shown to guarantee the closed-loop stability and asymptotic state tracking. It has also been shown that the proposed adaptive control allocation framework can reduce the controller complexity with proper grouping of the actuators. In this framework, the control signal to be allocated can be a non-adaptive controller designed with a conventional state feedback approach. This implies that the adaptive control allocation unit may be combined with a conventionally designed control loop for improved reliability. The proposed adaptive control allocation schemes have been applied to two linearized aircraft models. The simulation results have demonstrated the performance of the proposed algorithms and the applicability of the proposed schemes to aircraft flight control. Some future research topics in this direction include the extension of the adaptive control allocation framework to systems with multiple groups of actuators with failure compensation capability and adaptive grouping of the actuators, etc.

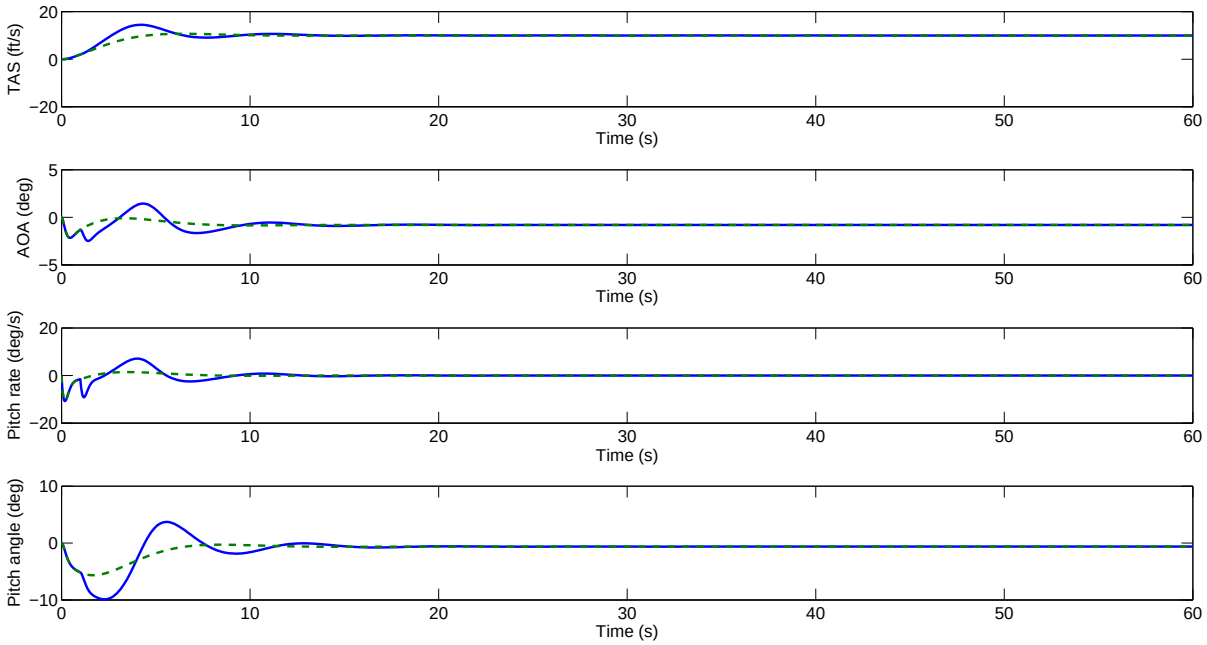

Figure 9. Time history of plant state (solid) and reference model state (dashed) (Case I).

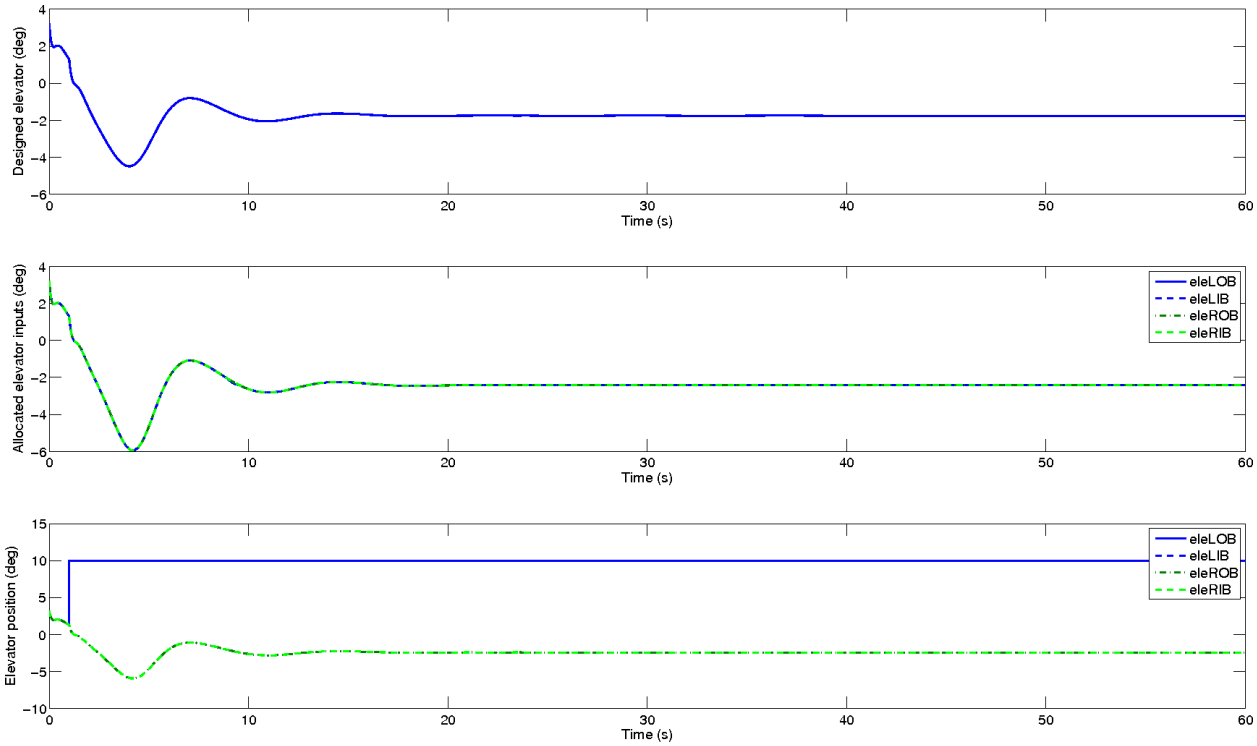

Figure 10. Time history of control signals and actuator outputs (Case I).

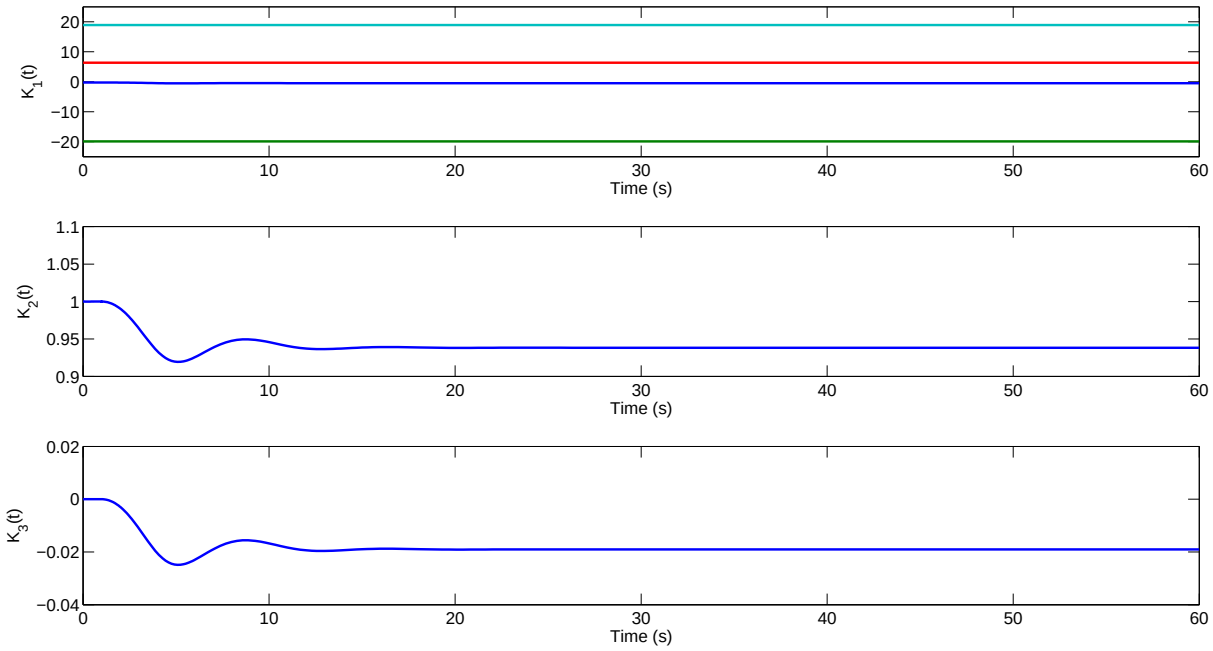

Figure 11. Time history of controller parameters (Case I).

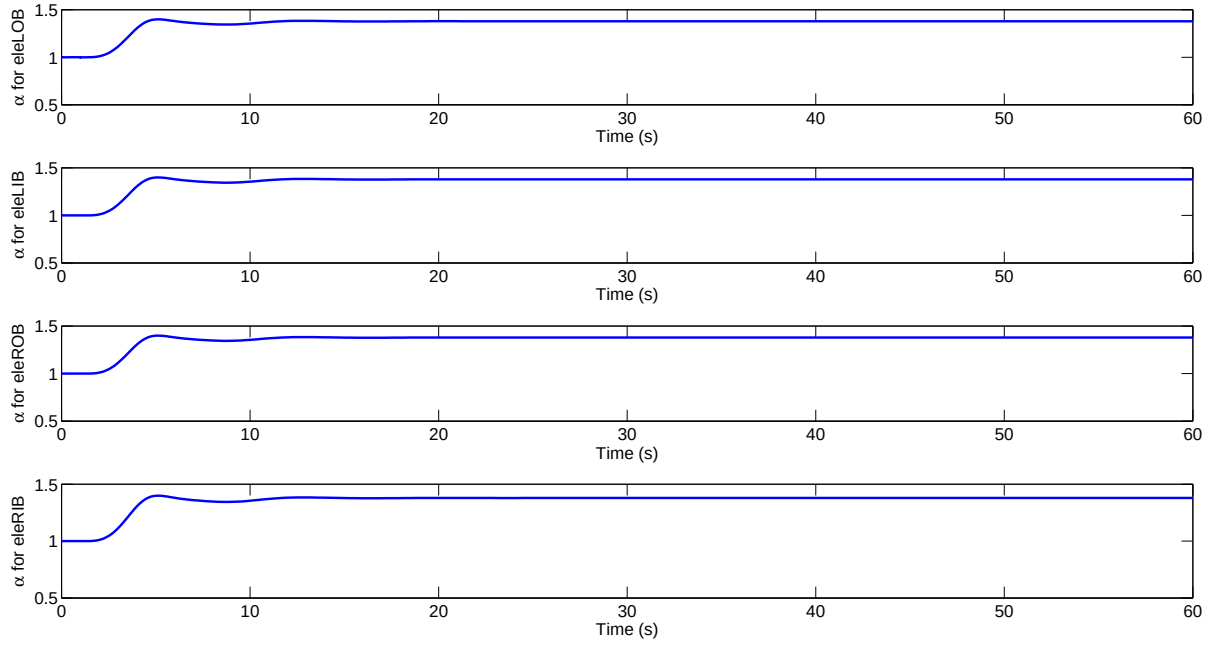

Figure 12. Time history of allocation gains (Case I).

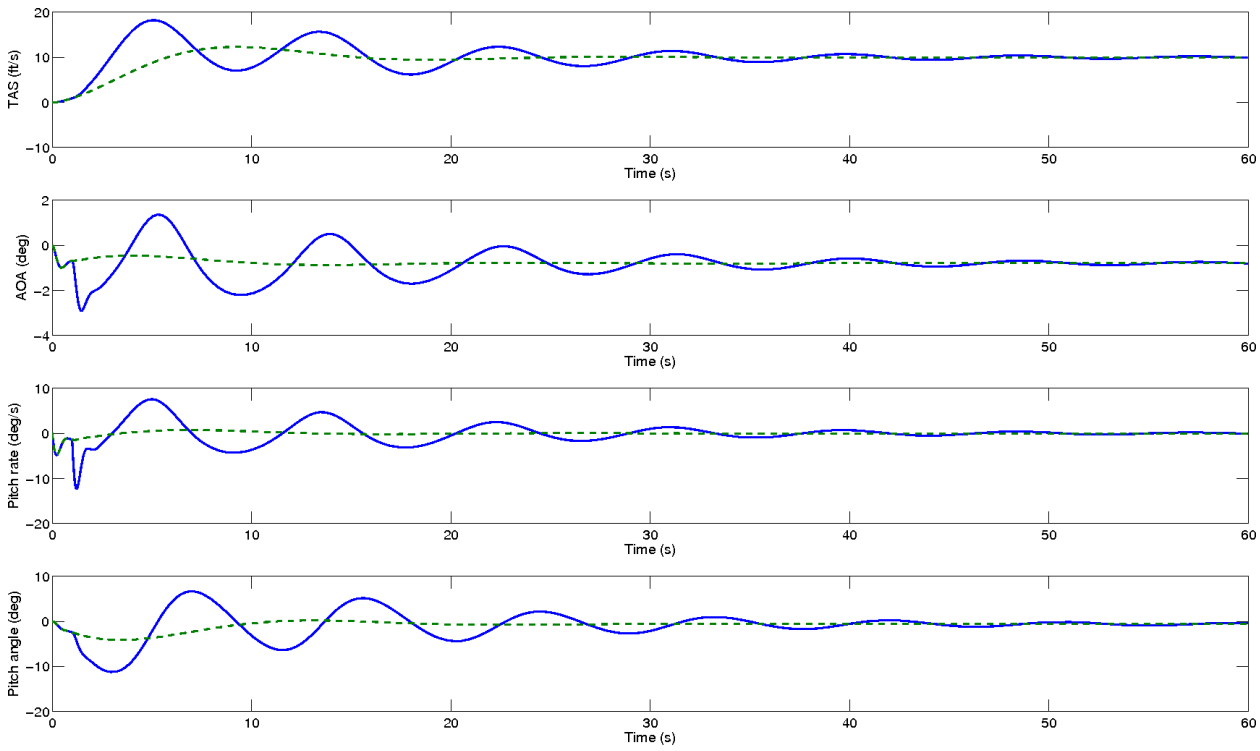

Figure 13. Time history of plant state (solid) and reference model state (dashed) (Case II).

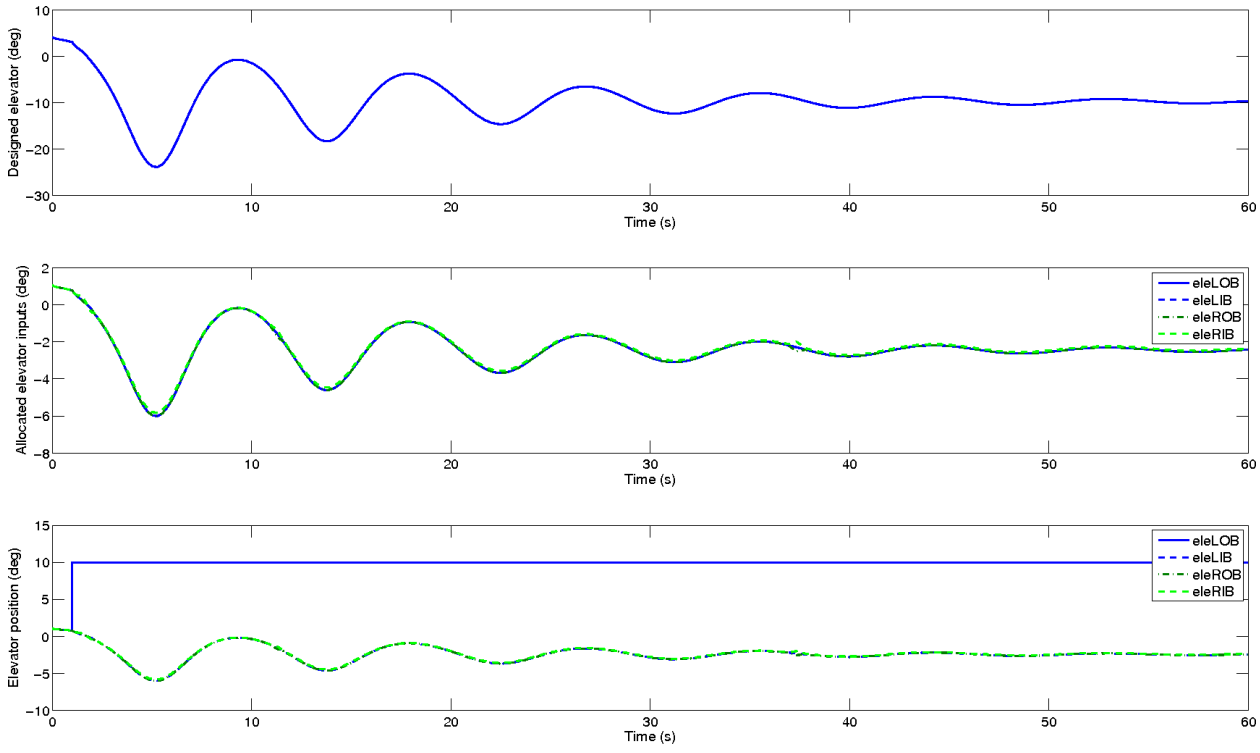

Figure 14. Time history of control signals and actuator outputs (Case II).

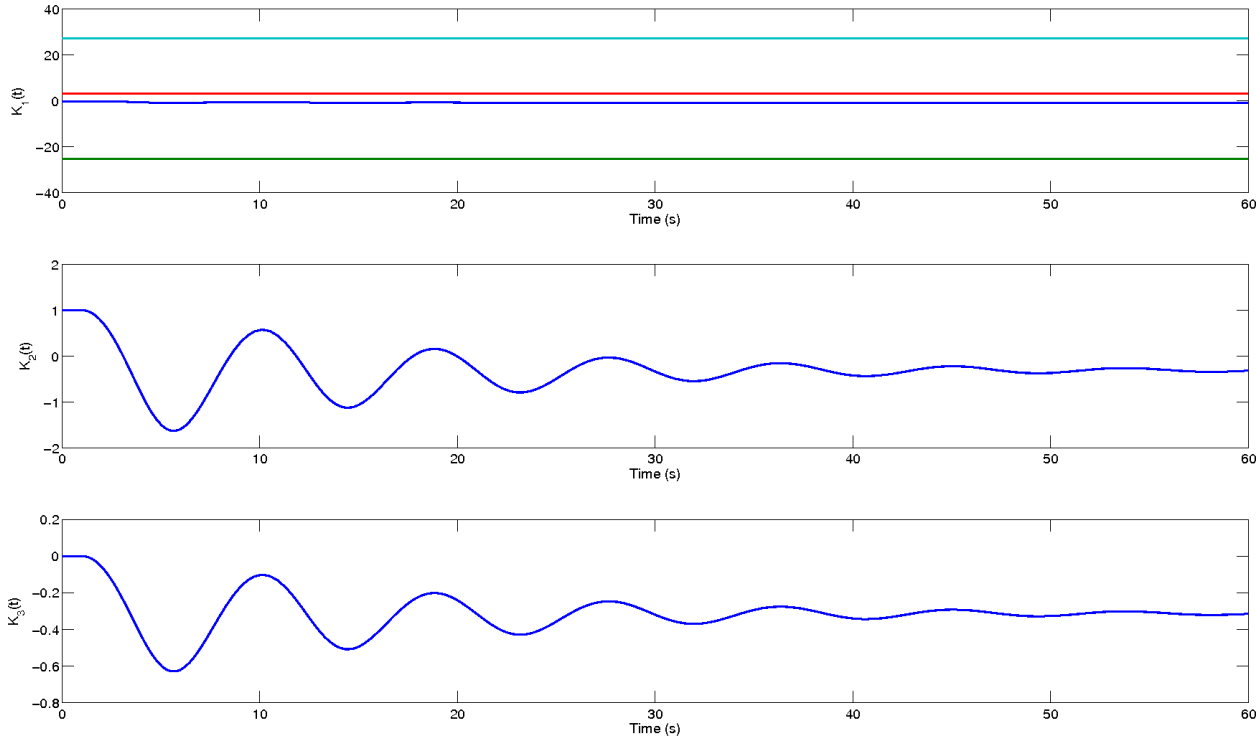

Figure 15. Time history of controller parameters (Case II).

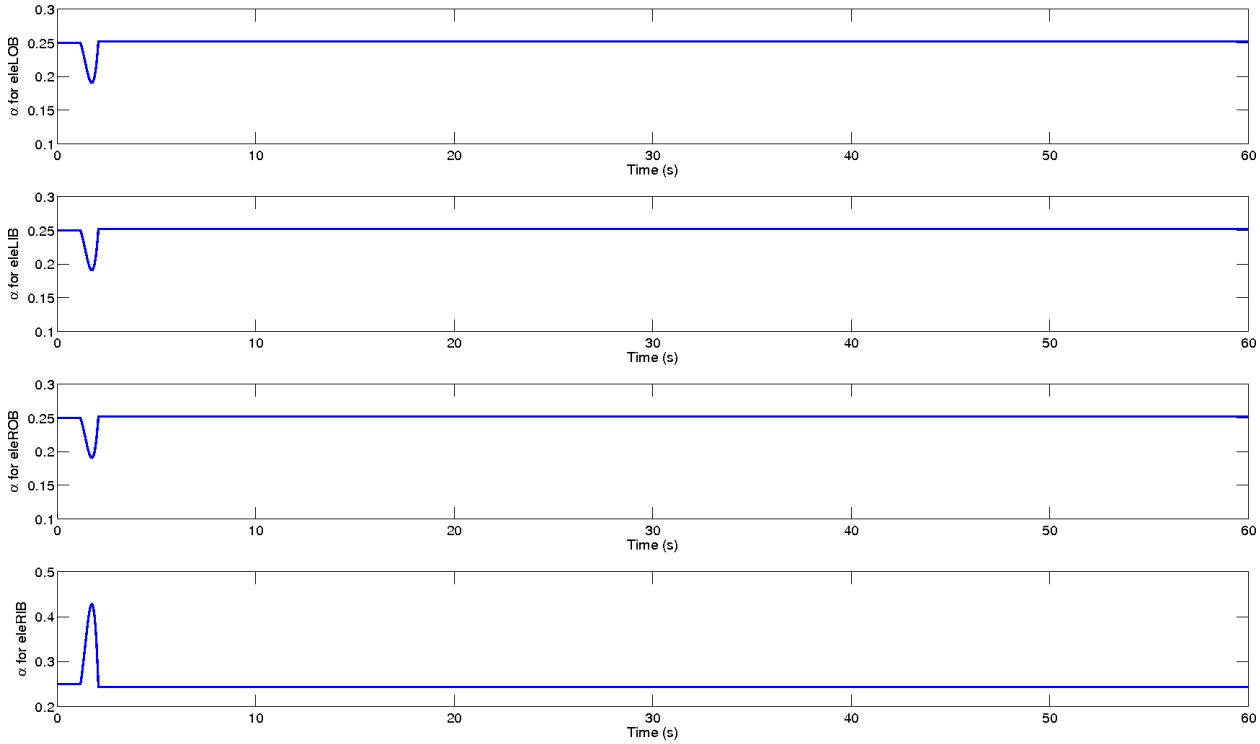

Figure 16. Time history of allocation gains (Case II).

Acknowledgment

This work was supported by the NRA NNX08AC62A of the IRAC project of NASA. The authors would like to thank Drs. Suresh M. Joshi and Sean P. Kenny at the NASA Langley Research Center for their valuable comments.

References

[1]Oppenheimer, M., Doman, D., and Bolender, M., "Control Allocation for Over-actuated Systems," *Mediterranean Conference on Control and Automation*, 2006, pp. 1–6.

[2]Buffington, J. M. and Enns, D. F., "Lyapunov stability analysis of daisy chain control allocation," *Journal of Guidance, Control, and Dynamics*, Vol. 19, November–December 1996, pp. 1226–1230.

[3]Davidson, J. B., Lallman, F. J., and Bundick, W. T., "Real-time adaptive control allocation applied to a high performance aircraft," 5*th SIAM Conference on Control and Its Applications*, 2001.

[4]Boskovic, J. D. and Mehra, R. K., "Multiple-model adaptive flight control scheme for accomodation of actuator failures," *Journal of Guidance, Control, and Dynamics*, Vol. 25, No. 4, 2002.

[5]Luo, Y., Serrani, A., Yurkovich, S., Oppenheimer, M. W., and Doman, D. B., "Model-predictive dynamic control allocation scheme for reentry vehicles," *Journal of Guidance, Control, and Dynamics*, Vol. 30, No. 1, January–February 2007, pp. 100–113.

[6]Venkataraman, R., Oppenheimer, M., and Doman, D., "A new control allocation method that accounts for effector dynamics," *2004 IEEE Aerospace Conference Proceedings*, 2004, pp. 2710–2715.

[7]Fahroo, F. and Doman, D., "A direct method for approach and landing trajectory reshaping with failure effect estimation," *Proceedings of 2004 AIAA Guidance, Navigation, and Control Conference*, No. AIAA-2004-4772, 2004.

[8]Bolender, M. A. and Doman, D. B., "Nonlinear control allocation using piecewise linear functions," *Journal of Guidance, Control, and Dynamics*, Vol. 27, No. 6, November–December 2004, pp. 1017–1027.

[9]Doman, D. B., Gamble, B. J., and Ngo, A. D., "Quantized control allocation of reaction control jets and aerodynamic control surfaces," *Journal of Guidance, Control, and Dynamics*, Vol. 32, No. 1, January–February 2009, pp. 13–24.

[10]Tao, G., Chen, S., Tang, X., and Joshi, S. M., *Adaptive Control of Systems with Actuator Failures*, Springer-Verlag, London, 2004.

[11]Crespo, L. G., Matsutani, M., Jang, J., Gibson, T., and Annaswamy, A., "Design and verification of an adaptive controller for the Generic Transport Model," *Proceedings of 2009 AIAA Guidance, Navigation, and Control Conference*, No. AIAA-2009-5618, Chicago, IL, August 2009.

[12]Liu, Y., Tang, X., Tao, G., and Joshi, S. M., "Adaptive compensation of aircraft actuation failures using an engine differential model," *to appear in IEEE Trans. on Control Systems Technology*, 2008.

[13]Tang, X., Liu, Y., and Tao, G., "A study of adaptation of multiple actuating signals for LTI systems," *Proceedings of 2006 American Control Conference*, June 2006, pp. 5996–6001.

[14]Jordan, T., Langford, W., Belcastro, C., Foster, J., Shah, G., Howland, G., and Kidd, R., "Development of a dynamically scaled generic transport model testbed for flight research experiments," *AUVSI's Unmanned Systems North America Symposium and Exhibition*, Anaheim, CA, August 2004.

[15]Jordan, T., Langford, W., and Hill, J., "Airborne subscale transport aircraft research testbed-aircraft model development," *Proceedings of AIAA Guidance, Navigation, and Control Conference*, No. AIAA-2005-6432, San Francisco, CA, August 2005.